



Numerical Simulation of Sandia D Flame Using Optimized k-e Transport Model-Based Eddy Dissipation Concept

Sumit Sagar Hota and Krishna Sesha Giri

EasyChair preprints are intended for rapid dissemination of research results and are integrated with the rest of EasyChair.

October 23, 2023

Numerical simulation of Sandia D flame using optimized k- ϵ transport model-based Eddy Dissipation Concept

Sumit Sagar Hota^{1,*}, Krishna Sesha Giri²

¹ Indian Institute of Technology Palakkad, Department of Mechanical Engineering, Palakkad, India

² Indian Institute of Technology Palakkad, Department of Mechanical Engineering, Palakkad, India

* 132114002@smail.iitpkd.ac.in

ABSTRACT

The aim of this study was to develop an efficient computational tool for transient reacting flows, specifically focusing on stationary flames. The tool was based on the Reynolds-averaged Navier-Stokes (RANS) equations and employed the k- ϵ turbulence model. The validation process involved using various single-step chemical kinetics models to simulate methane combustion in a Sandia D flame case. This simulation was carried out using the Eddy Dissipation Concept (EDC) within the OpenFOAM open-source Computational Fluid Dynamics (CFD) code. The findings from the validation revealed that the EDC model was the most effective choice for this application. Following this, the researchers applied several corrections to the k- ϵ model to further optimize the EDC model. Among these corrections, Pope's correction proved to be the most successful. Subsequent investigations delved into the variations within the EDC combustion model. After analyzing different versions, the EDC 81 model emerged as the most suitable for achieving accurate predictions as compared to any of the existing EDC models as proposed till date.

Keywords: EDC; k- ϵ model; Pope's correction; Sandia D

1 Introduction

In recent literature, the EDC [1] is very commonly employed in turbulent combustion modeling. However, the prediction of species & temperature profiles through EDC is not accurate enough [2 & 3]. The original EDC model of 1977 [4] was followed by several modifications that were proposed in the literature namely EDC 81 [5], EDC 96 [6], EDC 05 [7] (default EDC model on OpenFOAM [8]), EDC 16 [9] and EDC 17 [10]. This work aims to compare the various versions of the EDC model that have been proposed in past literature in predicting the structure of the Sandia Flame D [11] & [12] to identify the most suitable one. The Sandia D flame is chosen for comparison due to its widespread use as a reference flame in combustion research.

2 Numerical Methodology

2.1 IFC and EDM model

i. IFC (Infinitely Fast Chemistry Model)

The IFC (Infinite Fast Chemistry) model [4 & 13] runs on the concept that "mixed is burnt," which implies that it ignores any kinetic limitations on reaction speeds. It's crucial to keep in mind nevertheless that this model still doesn't directly account for turbulent characteristics like k and ϵ . Compared to other models, it has a computational advantage but is only applicable to situations requiring non-premixed flames. This model's basic assumption is that chemical equilibrium is attained more quickly than mixing occurs. The rate of consumption of fuel for the EDM model is given by given as:

$$\dot{\omega}_F = C \frac{\bar{\rho}}{\Delta t} \min \left[Y_F, \frac{Y_{Ox}}{s} \right] \quad (1)$$

ii. EDM (Eddy Dissipation Model)

A single-step global response mechanism is used by the Eddy Dissipation Model (EDM) [4], a combustion model. The dissipating rate of turbulent energy is taken into account while calculating the timing for chemical reactions. Turbulence mixing time scale ($\tau_{mix} = \frac{k}{\varepsilon}$), for EDM is a concern and was used for comparison with the chemical timescale. The fuel consumption rate for the EDM model is expressed as follows:

$$\dot{\omega}_F = C \bar{\rho} \frac{\varepsilon}{k} \min \left[Y_F, \frac{Y_{Ox}}{s} \right] \quad (2)$$

Where, $\dot{\omega}_F$, Y_F , Y_{Ox} , C , $\bar{\rho}$, ε , k , Δt & s represents the rate of fuel consumption or reaction, the mass fraction of fuel and oxidizer, the model constant, the mean flow density, the rate at which eddies dissipate energy, the rate at which turbulent kinetic energy is released, the time step, and the stoichiometric oxygen-to-fuel mass ratio.

2.2 EDC

In recent literature, the EDC is very commonly employed in turbulent combustion modeling. However, the prediction of species & temperature profiles through EDC is not accurate enough. This section compares the various versions of the EDC model that have been proposed in past literature in predicting the structure of the Sandia Flame D described later to identify the most suitable one.

The foundation of the EDC idea is the division of the computational cell into reacting and non-reacting zones. The typical response times are described by the following equations:

(a) EDC 1981

$$\bar{R}_i = \frac{\bar{\rho}}{\tau^*} \frac{\gamma_L^3 \chi}{1 - \gamma_L^3 \chi} (\bar{Y}_i - Y_i^*) \quad (3)$$

(b) EDC 1996

$$\bar{R}_i = \frac{\bar{\rho}}{\tau^*} \frac{\gamma_L^2 \chi}{1 - \gamma_L^3 \chi} (\bar{Y}_i - Y_i^*) \quad (4)$$

(c) EDC 2005

$$\bar{R}_i = \frac{\bar{\rho}}{\tau^*} \frac{\gamma_L^2 \chi}{1 - \gamma_L^2 \chi} (\bar{Y}_i - Y_i^*) \quad (5)$$

Further in the 2016 and 2017 versions of the EDC model additional relations as below are introduced.

(d) EDC 2016

$$C_\gamma = \frac{3C_{D2}^{\frac{1}{4}}}{4C_{D1}^2} \propto \sqrt{(Re_T + 1)Da_\eta} \quad (6)$$

$$C_\tau = \frac{C_{D2}^{\frac{1}{2}}}{3} \propto \frac{1}{Da_\eta \sqrt{Re_T + 1}} \quad (7)$$

(e) EDC 2017

$$C_\gamma = \left(\frac{3C_{D2}}{4C_{D1}^2} \right)^{\frac{1}{4}} = \sqrt{\frac{3}{2} (Re_T + 1) Da_\eta^{\frac{3}{4}}} \quad (8)$$

$$C_\tau = \left(\frac{C_{D2}}{3} \right)^{\frac{1}{2}} = \frac{1}{2 Da_\eta \sqrt{Re_T + 1}} \quad (9)$$

Where, Da_η , Re_T , C_γ , C_τ , C_{D1} and C_{D2} represents the Damköhler number at the Kolmogorov scale, the turbulent Reynolds number, local model constants, and constants related to the turbulent energy cascade.

$$Re_t = \frac{k^2}{\epsilon v} \quad (10)$$

$$\gamma_L = \left(\frac{3C_{D2}}{4C_{D1}^2} \right)^{\frac{1}{4}} \left(\frac{v\epsilon}{k^2} \right)^{\frac{1}{4}} = C_\gamma \left(\frac{v\epsilon}{k^2} \right)^{\frac{1}{4}} = C_\gamma Re_t^{-\frac{1}{4}} = (\gamma^*)^{\frac{1}{3}} \quad (11)$$

$$\tau^* = \left(\frac{C_{D2}}{3} \right)^{\frac{1}{2}} \left(\frac{\epsilon}{v} \right)^{\frac{1}{2}} = C_\tau \left(\frac{\epsilon}{v} \right)^{\frac{1}{2}} = C_\tau Re_t^{-\frac{1}{2}} \frac{k}{\epsilon} = \frac{\gamma^*}{\dot{m}} = \frac{1}{\dot{m}^*} \quad (12)$$

Where, k , ϵ , v and γ_L stand for turbulent kinetic energy, turbulent dissipation rate, and turbulent kinematic viscosity, as well as the fine structure length fraction of species i respectively. χ denotes the reacting fraction of the fine structures or the portion of the fine structure that participates in the reaction. As a generalization, it is assumed that this is unity.

Also, in the provided equation:

Y^* , τ^* - represent fine structure quantities for species mass fraction, residence time and density, respectively. \bar{Y} , $\bar{\rho}$ - represent cell-averaged quantities for species mass fraction and density, respectively.

The superscripts '*' and '-' are used to differentiate between fine structure values (which might provide more detailed information at a smaller scale) and cell-averaged values (which represent an average over a larger cell or volume). These distinctions are often made in computational fluid dynamics and other fields of science and engineering to account for variations in physical properties at different scales or resolutions

The average reaction rate for the 2016 & 2017 version of EDC is determined by applying Eqn. (5) with modified model constants during the calculation of γ_L Eqn. (11) and τ^* Eqn. (12). In the case of the 2016 version of EDC, both model constants are constrained to their default values, as illustrated as C_γ lower than 2.1377 and C_τ higher than 0.4083. Similarly, for 2017 version of the EDC model C_γ can be clipped to values that cannot be lower than the standard value of 2.1377 to avoid unreasonable late ignition and C_τ higher than 0.4083. For other EDC versions (1981, 1996, and 2005) default values of C_{D1} , C_{D2} , C_γ , and C_τ are 0.05774, 0.5, 2.1377, and 0.4083 respectively. Model constants like *exp1* have the values 3, 2, 2, 2 & 2 for EDC versions 1981, 1996, 2005, 2016, and 2017 respectively. Similarly, model constants like *exp2* have the values 3, 3, 2, 2 & 2 for EDC versions 1981, 1996, 2005, 2016, and 2017 respectively. The constants *exp1* and *exp2* are related by a scalar variable k (kappa) which takes both turbulence and chemistry interaction into account as represented in the following equation.

$$k = \frac{\gamma_L^{exp1}}{1 - \gamma_L^{exp2}} \quad (17)$$

2.3 Chemical Kinetics Mechanism

The simulation used in this work makes use of the GRI-Mech 3.0's [14] intricate chemical kinetic mechanism, which consists of 36 species and 219 elemental reactions. Although the original GRI-Mech 3.0 comprises 53 species and 325 elemental reactions, the simplified mechanism with 36 species is used in this study to specifically forecast NO species in methane-air combustion. Thermodynamic, transport, and reaction data obtained from CHEMKIN [15] are converted into the OpenFOAM file format using the chemkinToFoam tool.

2.4 OpenFOAM CFD code

The simulations in this study utilize two versions of the OpenFOAM CFD code, specifically Version 9 (v9) and Version 2206 (v2206). The solver employed for this research is reactingFoam, which is a time-dependent solver designed to simulate reactive systems with compressible characteristics, covering both laminar and turbulent flow scenarios. This solver utilizes stoichiometry expressions and reaction kinetic data to calculate the rates at which various chemical species are consumed and produced during reactions. Additionally, the solver can incorporate specific thermophysical models to obtain essential properties of the fluid mixture phase for accurate simulations. It is also equipped with various combustion models to effectively replicate turbulent combustion systems.

2.5 Sandia D flame and domain details

In this study, the typical Sandia D flame [14 & 15] is represented for methane-air combustion. The flame geometry consists of two concentric cylinders: the pilot jet emerges from the annulus, while the

main flow originates from the central cylinder. A schematic representation of the domain is shown in Figure 1. The primary jet has an exit velocity of 49.6 m/s and a temperature of 294 K because methane and air are combined there at a mole ratio of 1:3. The pilot jet, a combustion byproduct, has an exit velocity of 11.4 m/s and a temperature of 1880 K. In addition, a parallel jet of air moves at a speed of 0.9 m/s.

A two-dimensional, 5-degree sector is intended as the computing domain for simulations. At the intake of the main jet, pilot jet, and air jet, a zero gradient pressure condition is imposed to establish boundary conditions. At the outflow, total pressure boundary conditions are in effect. For the outlet velocity field, pressure inlet-outlet boundary conditions are used. Pressure and velocity wedge-type boundary conditions are defined for the wedge-shaped side surface of the domain. The computational region, representing the Sandia D flame, encompasses a specified main jet diameter (D) of 0.0072 meters. It extends from 0 to 0.15 meters in the radial jet orientation (equivalent to $r/D = 0$ to 20.833) and from 0 to 0.576 meters in the axial direction (equivalent to $x/D = 0$ to 80).

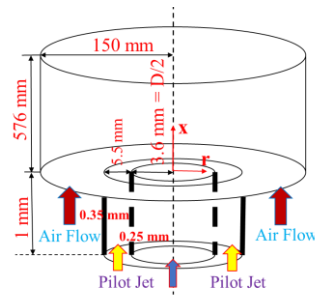


Figure 1: Schematic diagram of Sandia D flame

2.6 Mesh Independence analysis of Sandia D flame for EDC combustion model

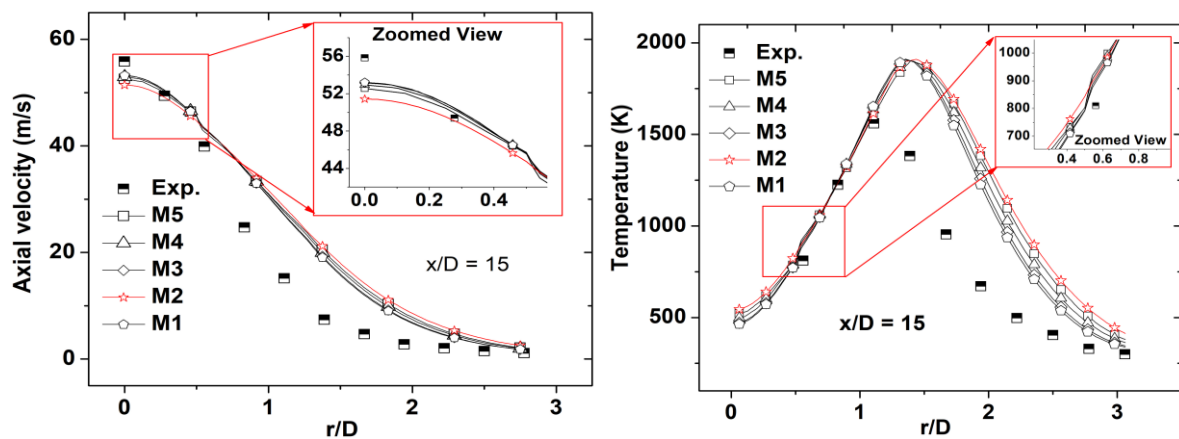


Figure 2: Mesh independence study plots of axial velocity vs. r/D at $x/D = 15$ (left) and temperature vs r/D at $x/D = 15$ (right).

Grid independence research was carried out starting with a cell count of at least 35608, designated as M5 in the Sandia D flame. The mesh was then refined by increasing the number of cells while maintaining a consistent aspect ratio of 1 in the region where the flame is established. The refined meshes are labeled as M4, M3, M2, and M1, with cell counts of 55510, 79812, 87144, and 108514, respectively. From the results presented in Figures 2, it may be observed that meshes M1 and M2 provided nearly identical predictions. As a result, M2 was found to be the most suitable mesh for the study. It's important to note that the maximum refinement occurred at the nozzle exit, with a grid spacing as fine as 0.3 mm, and the coarseness of the mesh increased towards the boundaries, reaching up to 1 mm.

3 Results and Discussion

3.1 Comparison of different combustion models using Sandia D flame

The EDC model, initially introduced by Magnussen et al. [4], introduced two fundamental models: EDM and IFC model. To understand the significance of the EDC model compared to these basic models (EDM and IFC), it is necessary to investigate their performance. Therefore, a comparison

between these basic models and the EDC 2005 or EDC (default) model with the default correction of Launder et al. [17] is conducted using the Sandia D flame validation case. This validation case involves a quadratic velocity profile with COD (Coefficient of Determination) as 0.9971 is implemented in the OpenFOAM code. The suitability and correctness of the EDC model for simulating the combustion process under the given conditions will be determined with the help of this comparison.

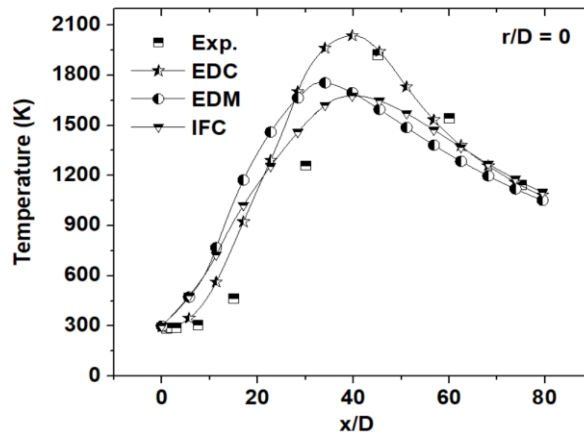


Figure 3: EDM, IFC, and EDC model comparison plots for Sandia D flame

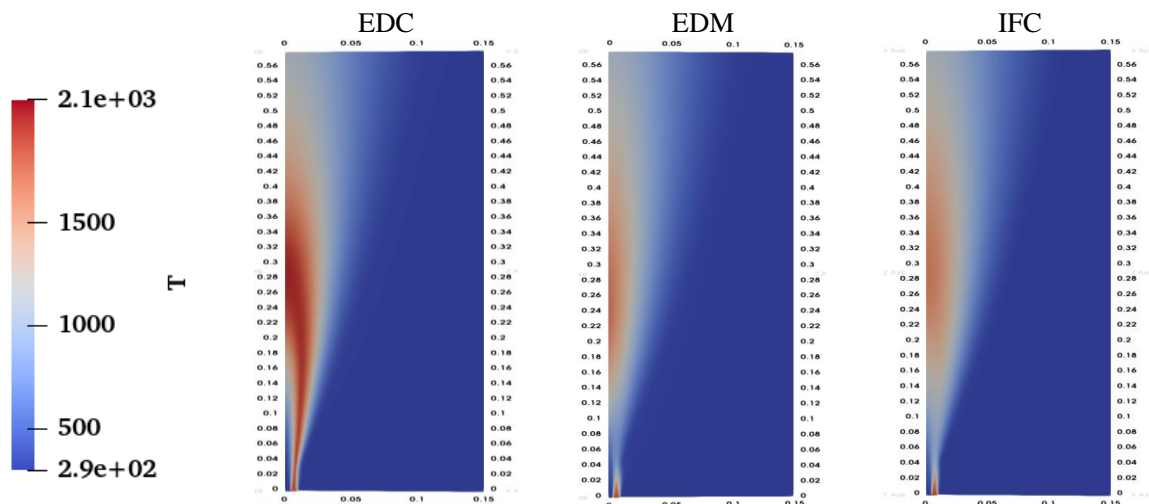


Figure 4: Temperature contours of EDM, IFC, and EDC model.

Figures 3 and 4 show a comparison of the EDC combustion model with the identical boundary conditions and beginning circumstances and the EDM and IFC combustion models with a single-step global reaction mechanism of methane combustion. The GRI-Mech 3.0 detailed kinetic mechanism is used by the EDC model.

Figure 3 shows that the EDC model frequently overestimates the peak temperature, which was found to be 2037.56 K with a minor leftward shift. However, when compared to experimental data, the actual peak temperature at $x/D = 45$ is 1922 K, while the EDC model predicts 1953.52 K. On the other hand, the EDM and IFC models significantly underpredict the peak temperature, with values of 1755.78 K and 1677.22 K, respectively. From Figure 4 it is clear that a single-step global reaction mechanism based on EDM and IFC shows flame extinction near the inlet with an axial position at $x/D = 5$ to 6 and $r/D = 1$ to 5. In conclusion, the EDC model offers a more precise forecast of the peak temperature, which is the region with the greatest temperature. It demonstrates an advantage of 52 K and 130 K compared to the EDM and IFC models, respectively, in capturing this critical temperature zone without flame extinction.

The reason of flame extinction is shown below:

In case of IFC combustion model flame extinction is due to the strain induced extinction. Thin mixing layers that are locally distorted and strained by the turbulent motion are where turbulent diffusion flames appear to be embedded. The local flow extinction may occur for sufficiently large strain rates, when the rate of mixing (or, equivalently, the rate of fuel burning per unit flame surface), is increased

above a critical value. Similarly in the case of EDM turbulence mixing time scale ($\tau_{\text{mix}} = k/\varepsilon$), was used for comparison with the chemical timescale. The weaker the flame near the injector, the more oxygen crosses the flame. This slightly changes the distribution of oxygen over the cross-section of the combustor.

To mitigate the problems associated with flame extinction, particularly in high-speed (supersonic) combustion scenarios, the EDC model with a finite rate chemistry model, such as quasi-laminar combustion theory, can be a suitable solution. This approach disregards the influences of temperature and component fluctuations on combustion, offering more stable results compared to the IFC model. Additionally, using the Kolmogorov timescale instead of the mixing timescale in the EDM can also help improve the results. This adjustment has shown marginal improvements in comparison to the previous approach. Thus, it can be claimed that the default EDC model with quadratic velocity profile is better than any of the single-step global reaction mechanism models like EDM and IFC models by a substantial margin (52 K and 130 K, respectively) when capturing this critical temperature zone at axial temperature plots.

3.2 Corrections in k- ε turbulent model

Launder's correction is the default correction utilized in the k- ε turbulent model. However, Figure 4 highlights a leftward shift in temperature plots. To evaluate the accuracy of the default correction in predicting the jet decay rate in velocity profiles, a study has been undertaken. This investigation utilizes a 7th-order velocity profile with a coefficient of discharge (COD) set to 1.00 for enhanced accuracy compared to the quadratic velocity profile. Within this study, 2005 is default version of the EDC is examined along with four different corrections: Pope (P) [16], Launder et al. (L) [17], Givi et al. (G) [18], and Chien (C) [19] as shown in Table 1. The objective of this analysis is to assess how effectively these various corrections simulate the decay rate of the jet in velocity profiles while avoiding a shift in the temperature profile.

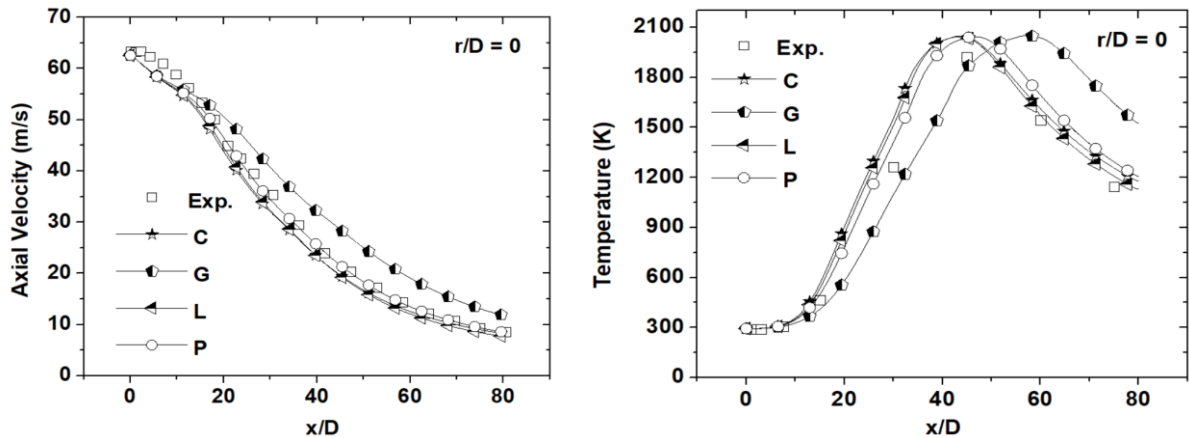


Figure 5: Investigation of the effect of correction for the k- ε turbulent transport model by plotting Axial velocity vs x/D at r/D = 0 (left) and Temperature vs x/D at r/D = 0 (right)

Table 1: Constants for correction to the k- ε standard model

Constants	C_μ	C_1	C_2	σ_k	σ_ε
P	0.09	1.45	1.90	1.0	1.3
L	0.09	1.44	1.92	1.0	1.3
G	0.09	1.52	1.9	1.0	1.3
C	0.09	1.35	1.8	1.0	1.3

As depicted in Figure 5 (left), the velocity profiles corresponding to various corrections exhibit distinct trends. In general, these corrections tend to slightly underestimate the experimental data from x/D = 0 to 10. However, the G correction is notable for its tendency to overpredict the velocity profile from x/D = 20 to 80 and its inability to accurately capture the jet decay rate. On the contrary, the L and C corrections closely resemble each other and consistently underestimate the results from x/D = 20 to 60. But the P correction shows good agreement with the outcomes of the experiment. With just a minor overprediction of outcomes in the region of x/D = 20 to 40, it coincides well with the experimental data from x/D = 40 to 80. Notably, the peak velocity at r/D = 0 is nearly the same for all

corrections, with an average value of under prediction of 0.87 m/s. This is in comparison to the experimental prediction of 63.43 m/s.

In Figure 5 (right), the temperature profiles for various corrections are presented. Except for the G correction, all other corrections tend to overpredict the peak temperature, with an average overprediction of 124 K. However, at $x/D = 45$, which corresponds to the experimental peak temperature of 1922 K, the G correction significantly underestimates the temperature, yielding a value of 1859.4 K. This is due to a rightward shift of the temperature peak to $x/D = 57$ instead of $x/D = 45$. Similarly, there is a slight leftward shift of the temperature peak for the C and L corrections to $x/D = 43.6$. The P correction exhibits a slight rightward shift of the peak to $x/D = 46.72$, but it generally captures the trend of experimental results at nearly every data point.

To sum it up, the combination of Pope's (P) correction with the default EDC 2005 combustion model and a 7th-order velocity profile stands out as the superior choice. This model, while slightly overpredicting peak temperature by 124 K and underpredicting velocity by 0.87 m/s, excels in delivering a quantitative assessment of vortex stretching effects and accurately predicting jet decay rates compared to other existing models. Consequently, this model represents an exceptional combination that outperforms all default EDC models with their standard corrections in the $k-\epsilon$ model.

3.3 Comparison of different versions of EDC

The EDC 2005 version is the default version of the EDC combustion model used for conducting simulations in the OpenFOAM code. There are different versions of the EDC model depending on different years, such as EDC 1981, 1996, 2005, 2016, and 2017. After the 2017 EDC version, there have been modifications to the EDC model as reported in the literature. Figure 5 indicates a temperature overprediction of 124 K for the default EDC 2005 model, even though the velocity profile with Pope's correction is well-predicted. As a result, it is crucial to look at the predictions of temperature, velocity, and major species predictions.

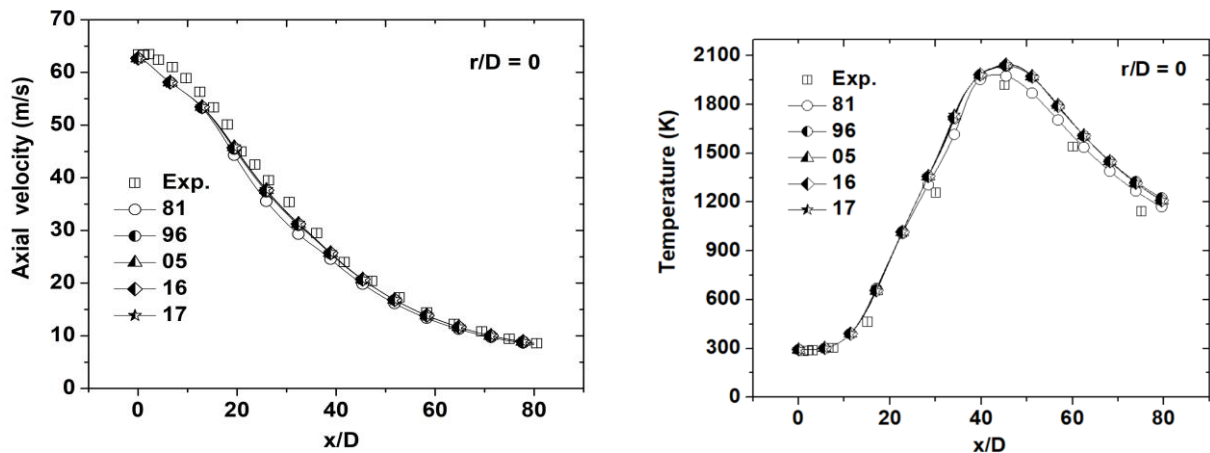


Figure 6: Comparison of different versions of EDC for axial velocity vs. x/D at $r/D = 0$ (left) and temperature vs. x/D at $r/D = 0$ (right)

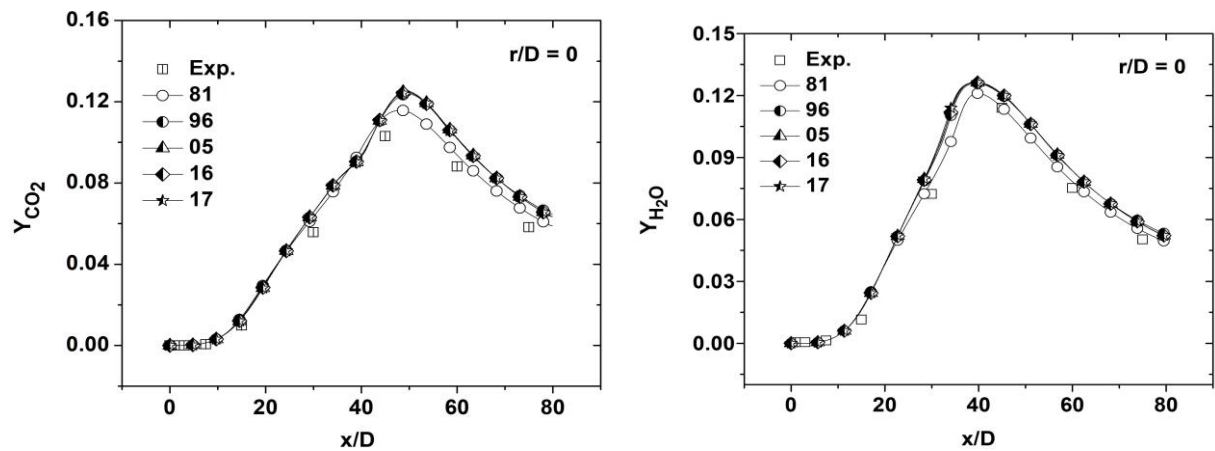


Figure 7: Y_{CO_2} vs x/D (left) & Y_{H_2O} vs x/D (right) at $r/D = 0$ for different EDC versions

In Figures 6 & 7, the 7th-order velocity profile of Sandia D flame through the k- ϵ turbulent transport model using Pope's correction in a uniformly refined mesh is implemented in EDC combustion models. The notation used signifies that 81: EDC 1981, 96: EDC 1996, 05: EDC 2005, 16: EDC 2016, 17: EDC 2017.

It is clear from a comparison of the experimental data in Figure 6 (left) that all of the EDC models, from $x/D = 40$ to 80 , achieve good agreement with the tests. However, from $x/D = 20$ to 40 , EDC 16 and EDC 17 exhibit the best results, slightly surpassing EDC 1981. This improved performance in EDC 16 and EDC 17 can be attributed to the zone from $x/D = 20$ to 40 , where mixtures burn intensely, causing a dramatic rise in flow velocity and temperature. These models incorporate variables C_τ and C_γ , allowing in order to more accurately depict the shifting average reaction rate. In this context, decreasing C_γ is necessary to reduce the mean reaction rate. It's worth noting that the peak velocity profile of EDC 81 is slightly better than other models, with a value of 62.6581 m/s (i.e., 0.7719 m/s under prediction as compared to experimental data). In comparison, the other EDC models, namely EDC 96, EDC 05, EDC 16, and EDC 17, have peak velocity profiles of 62.6423 m/s, 62.6562 m/s, 62.6532 m/s, and 62.6353 m/s, respectively. These velocities are in contrast to the experimental velocity profile of 63.43 m/s, which is approximately at $x/D = 0$.

Inconsistencies in temperature are visible in the peak temperature zone, where potent mixes burn, according to the temperature profiles in Figure 6 (right). Every time, the EDC 1981 model performs better than the competition. One of the key reasons for the significant over-prediction of mean temperatures in the other EDC models is the overestimation of the mean reaction rate, which should be adjusted according to Eqn. (3) of the EDC 1981 model. For instance, at the peak temperature point at $x/D = 45$ and $r/D = 0$, the temperature values for the EDC 81 model have 56 K overprediction of temperature as compared to the experimental temperature of 1922 K. Consequently, the other EDC model demonstrates an average overprediction of 3.2% in predicting peak temperature as compared to the EDC 81 model.

For the mean mass fraction of CO_2 , some over-predicted values along the axial ($r/D = 0$) direction are found in all the cases of the EDC model. EDC 81 has shown the best estimation of results in axial directions with a peak reduction mean mass fraction of CO_2 , which is only possible by changing EDC constants in the EDC model & successfully done by the EDC 81 model. Similarly, for H_2O mean mass fraction shows slight prediction in the axial ($r/D = 0$) direction for the EDC 81 model and acts as the best-predicted model as compared to other EDC models.

Figure 7 (left) shows that, in contrast to experimental expectations, the peak of the mean mass fraction of CO_2 for all the EDC models is shifted to the right. Specifically, the peak mean mass fraction for the EDC 81 model is overpredicted with a value of 0.013 as compared to experimental results of 0.103 . In addition, the other EDC models achieve an average overprediction of 7.5% in predicting the peak mean mass fraction of CO_2 as compared to the EDC 81 model. Similarly, Figure 7 (right) reveals a left-side shift of the peak in comparison to experimental predictions for the mean mass percent of the H_2O trend for all EDC models. The EDC 81 model's peak mean mass fraction overpredicts by 0.007 compared to experimental observations, which provide a value of 0.114 . Here again, other EDC models demonstrate an average over-prediction of 4% in predicting the peak mean mass fraction of H_2O as compared to the EDC 81 models. The reason for the overpredictions of CO_2 and H_2O mean mass fraction is because of model constants of EDC model which in turn is due to the mean reaction rate of EDC models.

In summary, the EDC 81 model's predictions for velocity trends are highly accurate even without any modifications to the model variables C_τ and C_γ . Notably, it achieves the best peak velocity prediction of 62.6581 m/s, surpassing all other EDC models. Furthermore, in terms of temperature predictions, the peak temperature of 1978 K exhibits the least over-prediction ever observed in any combustion model, with an almost perfect alignment of the axial temperature profile. Additionally, the EDC 81 model excels in predicting the mean mass fractions of CO_2 and H_2O , with only slight over-predictions of 0.013 and 0.007 , respectively. This minimal over-prediction in temperature and species concentrations can be attributed to the EDC 81 model's mean reaction rate, which represents the smallest degree of over-prediction observed to date.

4 Conclusion

Based on the comprehensive analysis presented above, several significant findings emerge:

1. The default EDC model with a quadratic velocity profile outperforms single-step global reaction mechanism models like EDM and IFC models by a considerable margin, displaying a clear advantage of 52 K and 130 K in accurately predicting the critical temperature zone in axial temperature plots.
2. When combined with the default EDC 2005 combustion model and a 7th-order velocity profile, Pope's (P) correction proves to be the most effective among all possible corrections in the k- ϵ transport model. Although this combination slightly overpredicts peak temperature by 124 K and underpredicts velocity by 0.87 m/s, it excels in quantitatively assessing vortex stretching effects and accurately predicting jet decay rates. Consequently, this proposed model represents an exceptional combination that surpasses the capabilities of any default EDC models with their standard corrections in the k- ϵ model.
3. The EDC 81 model delivers highly accurate predictions for velocity trends, achieving the best peak velocity prediction of 62.6581 m/s among all EDC models. It also excels in temperature predictions, with the least overprediction of peak temperature (1978 K) ever observed in any combustion model and nearly perfect alignment of the axial temperature profile. Moreover, the EDC 81 model effectively predicts the mean mass fractions of CO₂ and H₂O, with only slight overpredictions of 0.013 and 0.007, respectively.

In summary, the optimized EDC model, particularly the EDC 81 version, stands out as the best among the EDC models investigated in this research, as exemplified by its exceptional performance in predicting velocity and temperature profiles. To further enhance this highly optimized EDC model, the future work of this research will explore the implementation of the modified EDC (MEDC) approach.

References

- [1] Markus Bösenhofer, Eva-Maria Wartha, Christian Jordan and Michael Harasek, “The Eddy Dissipation Concept—Analysis of Different Fine Structure Treatments for Classical Combustion”, *Energies* 2018, 11, 1902; doi:10.3390/en11071902.
- [2] Farokhi, M.; Birouk, M. Application of Eddy Dissipation Concept for Modeling Biomass Combustion, Part 1: Assessment of the Model Coefficients. *Energy Fuels* 2016, 30, 10789–10799.
- [3] Farokhi, M.; Birouk, M. Application of Eddy Dissipation Concept for Modeling Biomass Combustion, Part 2: Gas-Phase Combustion Modeling of a Small-Scale Fixed Bed Furnace. *Energy Fuels* 2016, 30, 10800–10808.
- [4] Magnussen, B.F.; Hjertager, B.H. On mathematical modeling of turbulent combustion with special emphasis on soot formation and combustion. *Symp. Int. Combust.* 1977, 16, 719–729.
- [5] Magnussen, B.F. On the structure of turbulence and a generalized Eddy Dissipation Concept for chemical reaction in turbulent flow. In *Proceedings of the 19th Aerospace Sciences Meeting*, St. Louis, MO, USA, 12–15 January 1981.
- [6] Gran, I.R.; Magnussen, B.F. A Numerical Study of a Bluff-Body Stabilized Diffusion Flame. Part 2. Influence of Combustion Modeling And Finite-Rate Chemistry. *Combust. Sci. Technol.* 1996, 119, 191–217.
- [7] Magnussen, B.F. The Eddy Dissipation Concept—A Bridge Between Science and Technology. In *Proceedings of the ECCOMAS Thematic Conference on Computational Combustion*, Lisbon, Portugal, 21–24 June 2005.
- [8] <https://www.OpenFOAM.com/>
- [9] Parente, A.; Malik, M.R.; Contino, F.; Cuoci, A.; Dally, B.B. Extension of the Eddy Dissipation Concept for turbulence/chemistry interactions to MILD combustion. *Fuel* 2016, 163, 98–111.
- [10] Bao, H. Development and Validation of a New Eddy Dissipation Concept (EDC) Model for MILD Combustion. Master’s Thesis, Delft University of Technology, Delft, The Netherlands, 2017.
- [11] R. S. Barlow and J. H. Frank, Effect of turbulence on species mass fraction in methane/air jet flames. Combustion Research Facility Sandia National Laboratories Livermore, CA 94551-0969, USA, Twenty-Seventh Symposium (International) on Combustion/The Combustion Institute, 1998/pp. 1087–1095.
- [12] Barlow, R., & Frank, J. (Year). Piloted CH₄/Air Flames C, D, E, and F – Release 2.1. Sandia National Laboratories. Retrieved from <http://www.ca.sandia.gov/TNF>
- [13] Fikri, D. R. A. (2017). Modeling Non-premixed Turbulent Combustion in Industrial Rotary Kiln: Application in OpenFOAM.
- [14] Smith, G.P., Golden, D.M., Frenklach, M., Moriarty, N.W., Eiteneer, B., Goldenberg, M., Bowman, C.T., Hanson, R.K., Song, S., Gardiner, W.C., Lissianski, V.V., and Qin, Z. 1999. Detailed chemical kinetic mechanism for methane combustion. Available at: http://www.me.berkeley.edu/gri_mech/version30/text30.html
- [15] Kee, R.J., Rupley, F.M., and Miller, J.A. 1991. Chemkin-II: A Fortran chemical kinetics package for the analysis of gas-phase chemical kinetics. Sandia Report SAND89-8009B, Sandia National Laboratory, Livermore, CA.
- [16] S. B. Pope, An Explanation of the Turbulent Round-Jet/Plane-Jet Anomaly, Imperial College, London, England, March 1978.
- [17] B.E. Launder and D.B. Spalding, The numerical computation of turbulent flows, Imperial College of Science and Technology, Department of Mechanical Engineering, Exhibition Road, London, S, W.7 , UK, *Computer methods in applied mechanics and engineering* 3(1974) 269-2890 north-holland publishing company.
- [18] P. Givi and J. I. Ramos, On the calculation of heat and momentum transport in a round jet, Department of Mechanical Engineering Carnegie-Mel Ion University Pittsburgh, Pennsylvania 15213, U.S.A. *Int. comm. Heat mass transfer* Vol. ii, pp. 173-182, 1984.
- [19] Kuei-Yuan Chien, Predictions of Channel and Boundary-Layer Flows with a Low-Reynolds-Number Turbulence Model, VOL. 20, NO. 1, JANUARY 1982, AIAA800134R, AIAA JOURNAL.